Design of 7 wt.% Y_2O_3-ZrO_2/Mullite Plasma-Sprayed Composite Coatings for Increased Creep Resistance

Elizabeth Withey[1], Christopher Petorak[1], Rodney Trice[1]

[1]School of Materials Engineering, Purdue University, West Lafayette, Indiana 47907-2044

Graeme Dickinson [2] and Thomas Taylor[2]

[2]Praxair Surface Technologies Inc., Indianapolis, Indiana 46224

This work was supported by the National Science Foundation through DMR-0134286 and by a donation from Praxair Surface Technologies Inc.

Prepared for the Journal of the American Ceramic Society

Abstract

Plasma-sprayed stand-alone coatings of 7 wt.% Y_2O_3-ZrO_2 (YSZ), nominally 74 wt.% Al_2O_3-26 wt.% SiO_2 mullite, and a 45:55 volume ratio composite of YSZ to mullite were examined using X-ray diffraction, dilatometry, and compression creep. Creep test were conducted on all three coating types in the as-sprayed condition at stresses from 40-80 MPa and temperatures of 1000° – 1200°C. The linear thermal expansion of YSZ/Mullite composite specimens was 6.4 x 10^{-6}/°C. While the creep behavior of YSZ/mullite composite specimens was between that of pure YSZ and pure mullite specimens for all combinations of temperature and stress tested, the creep response of the composite was more similar to that of pure mullite for all cases tested, consistent with mullite being the continuous phase in the composite.

I. Introduction

Thermal barrier coatings (TBCs) are commonly used to protect metallic components of turbine engines that could melt or oxidize at high service temperatures.[1,2,3,4,5,6,7,8,9] Most TBC systems consist of a ceramic top coat plasma-sprayed onto an intermetallic bond coat attached to a superalloy substrate. Yttria-stabilized zirconia (7 wt.% Y_2O_3-ZrO_2 or YSZ) is commonly used as the ceramic top coat in these systems because of its high melting temperature (~2700º C) and low thermal conductivity (~2 W/m/K);[1] a 200 μm thick coating of YSZ can decrease the surface temperature of a metallic component by up to 200ºC.[2,5] This insulative layer can increase the efficiency and/or lifetime of key turbine engine components by affording higher operating temperatures and/or by decreasing the temperature of metallic engine components.[6,7]

In the as-sprayed state, YSZ coatings have a lamellar microstructure with columnar grains perpendicular to the substrate along with intralamellar cracks and interlamellar pores.[3,6,7] Upon heating, the combustion of the fuel exposes the top surface of the YSZ coating to temperatures of 1200º-1300º C.[4,10] A thermal gradient is established through the thickness of the YSZ coating due to its low thermal conductivity and the transient heating, which results in a biaxial compressive stress gradient through its thickness.[8,11] Kokini and others have shown that coatings almost immediately begin to relax this stress.[11,12,13,14,15,16] On cooling, a tensile stress gradient through the thickness of the coating develops in proportion to the amount of in-service relaxation that occurred. This tensile gradient can lead to through thickness cracks in the coating, which can eventually cause spallation and failure of the coating.[11]

If the amount of coating relaxation during initial heating is reduced, the magnitude of the tensile stress in the coating during cooling should decrease. In the following work, a two-phase composite coating was designed, fabricated and evaluated with the overall purpose to reduce its

creep response in compression. A blend of YSZ and mullite phases was chosen for this new topcoat. The thermal properties of both materials are compared in Table 1. [17] Mullite was chosen for its excellent creep resistance[18,19]. Kokini et al.[15] predicted using analytical models that mullite did relax less than YSZ at high temperatures. In their models, they showed that coatings of mullite did not form through thickness cracks on cooling, whereas YSZ coatings did under the same conditions. Yoon et al. [20] have shown that rigid mullite inclusions in a 2 wt.% tetragonal YSZ decreased the creep rate of zirconia/mullite composites with increasing volume fraction of mullite up to 50 %. However, mullite has a lower coefficient of thermal expansion (CTE) and a higher thermal conductivity than YSZ, which could be detrimental to the new coating design by increasing the CTE mismatch between coating and substrate and reduce its ability to protect the underlying metallic structure.

In this study, a composite thermal barrier coating made from a combination of YSZ and mullite was investigated. Powders of each phase were mechanically mixed together, sprayed and stand-alone coatings were formed. These coatings were compression creep tested at temperatures of 1000^{o} through 1200^{o}C and stresses of 40 to 80 MPa. The goal was to design a coating system that crept less in compression than the industry standard thermal barrier coating, 7 wt.% Y_2O_3-ZrO_2.

II. Experimental Procedures

(1) Sample Preparation

YSZ, mullite, YSZ/mullite composite coatings were fabricated by air-plasma spraying spray-dried 7 wt. % Y_2O_3-ZrO_2 (~82 μm), fused and crushed mullite (~100 μm), and a mechanically mixed combination of the two powders onto a 12.7 mm diameter hollow aluminum rod (Praxair Surface Technologies (PST), Indianapolis, IN). YSZ coatings were sprayed using a

PST 1108 torch and the mullite and composite coatings with a Metco F4 torch. Coatings were sectioned into ~17 mm specimens using the procedure specified by Dickinson et al.[12] The aluminum substrate was removed using a 40% aqueous HCl solution, after which specimens were ultrasonically cleaned in deionized water. The outer diameter of each specimen was measured prior to dissolving the aluminum rod. The inner diameter of the coatings was assumed to be the same as the outer diameter of the aluminum rod.

(2) Physical Characterization

SEM Characterization: SEM micrographs of the polished surface of an as-sprayed composite specimen in cross-section were taken, as well as fracture surfaces of as-sprayed YSZ, composite, and mullite specimens. Micrographs were taken with a Hitachi S4800 FESEM using an accelerating voltage of 5 keV. The volume fraction of each phase in the composite was determined using a point-count method on the cross-sectional micrographs of the polished composite.

Density Measurements: Archimedes' method was used to determine the bulk density of each coating specimen after ultrasonic cleaning. The total porosity of the coatings was calculated using theoretical densities of 3.18 and 6.08 g/cm^3 for mullite and YSZ, respectively.[21,22] The theoretical density of the composite coatings was determined using an upper bound rule-of-mixtures approach employing the theoretical densities of YSZ and mullite. As stated previously, the volume fractions of YSZ and mullite in the composite coatings were determined from SEM micrographs using the point count method.

Thermal Expansion Measurements**:** Using cylindrical specimens, the average in-plane coefficient of thermal expansion (CTE) each coating type was determined by testing three or more coatings using a dilatometer (Orton Dilatometer Model 2016STD). Each specimen was heated at 5°C/min to 1200°C while simultaneously recording the change in height as a function of temperature. The CTE of each specimen was determined between 200°-550°C for mullite and composite specimens, and between 200°-800°C for YSZ specimens. These regions corresponded to the most linear response of the coating. The predicted CTE of the composite coating was again calculated employing a rule of mixtures using the measured volume fractions of YSZ and mullite.

Phase Analysis: X-ray diffraction [a] (XRD) was performed on pulverized mullite specimens over 2θ values of 20^{o}-80^{o} in the as-sprayed condition and after a 50-hour heat treatment at 1400°C in air. A scan rate of 10°/min with a step size of 0.05° was used.

(3) Creep Testing

Creep Testing Procedure: The in-plane creep behavior of YSZ, mullite, and the composite stand-alone coatings was measured using a servo-hydraulic load frame (MTS 810) outfitted with hydraulic collet grips (MTS 646 and an alignment fixture (MTS 609), a 100 kN force transducer, SiC pushrods, and a high-temperature furnace (Applied Test Systems, Inc.). Strain was measured using a high-temperature extensometer (MTS 632.70H-01) with a resolution of ± 1 μm. The extensometer consisted of an alumina pushrod that extended vertically through the center of the lower SiC pushrod platen and the hollow stand-alone coating. Strain was

[a] Siemens Kristalloflex Diffraktometer 500 using Cu-K_{α} radiation

determined by measuring the displacement between the upper stationary SiC platen and the cantilever supporting the alumina pushrod. [13]

Before load was applied, specimens were heated at 10 °C/min to 1000°, 1100°, or 1200ºC and allowed to equilibrate for 15 minutes. Specimens were then loaded in compression at 20 N/s to stresses of 40, 60, or 80 MPa and held for 5 hours. While past researchers have crept YSZ coatings for as long as 70 hours using similar cylindrical geometries[23], our initial creep investigations of mullite and YSZ/mullite composite coatings were intentionally kept short so that more testing conditions and replicates could be evaluated. Further studies would be needed to isolate the long term creep behavior of mullite and YSZ/mullite coatings.

Sample variability was determined by testing three of each coating type at 40 MPa and 1000° and 1200°C. This was established to be ±0.09% and ±0.03% strain for YSZ and mullite coatings, respectively, independent of the test temperature. For composite coatings the variability was ±0.05% strain at 1000°C and ±0.15% strain at 1200°C. Small variations in the initial elastic strain across materials and individual coatings of the same material were attributed to differences in porosity of each specimen. Thus, before comparing the plastic creep behavior of each stand-alone coating the elastic strain was subtracted.

Characterization of Creep Behavior: Within the limited time frame of the creep test, each sample demonstrated an apparent steady-state strain rate that was calculated from the slope of the linear portion of the creep data between 10,000 and 17,000 seconds. Comparison of these rates for each coating type will provide a basis for evaluating differences in coating response to combinations of stress and temperature. These apparent steady-state stress rates, $\dot{\varepsilon}_{ss}$, were also used to determine the activation energy for each coating type according to:

$$\dot{\varepsilon}_{ss} = A\sigma^n e^{-\frac{Q}{RT}} \quad [5]$$

where A is a material dependent constant, σ the applied stress, n the stress exponent, Q the creep activation energy in kJ/mol, R the universal gas constant (8.314 J/mol/K), and T the test temperature in Kelvin.[24] For specimens that failed during the creep test, the steady-state strain rate was calculated from the linear portions of the data prior to the rapid increase in strain.

III. Results and Discussion

(1) As-Sprayed Microstructure

The average amount of mullite in the composite coating was found to be 54±4 vol.% from 7 images taken randomly throughout one composite specimen. An example of an image analyzed is shown in Figure 1. The calculated theoretical density of the YSZ/mullite composite based on these measurements is presented in Table 2 along with the theoretical densities of YSZ and mullite and the average bulk densities and total porosities of each type of coating. Total porosity was highest in the mullite and YSZ/mullite composite specimens.

Fracture surfaces of as-sprayed coatings revealed a stacked lamellar pattern with interlamellar pores and intralamellar cracks in YSZ coatings, and in the YSZ regions of the composite coatings (Figure 2). Both of these coatings also showed columnar YSZ grains perpendicular to lamellae length (Figure 2a and b). The fracture surface of the mullite specimen appeared to be glassy (Figure 2c) as has also been observed by Ramaswamy et al.[2] This was confirmed using XRD (see Figure 3) where as-sprayed mullite specimens showed an amorphous background and 50-hr heat treated specimens showed well defined peaks. Distinct regions of crystalline YSZ and glassy mullite were observed in the composite coating (Figure 2b).

(2) Coefficient of Thermal Expansion

As shown in Figure 4, all three coatings exhibited an approximately linear thermal expansion upon heating. For YSZ, this behavior was consistent across the entire temperature range, whereas mullite and composite specimens showed dramatic shrinkage at ~970°C. This shrinkage was due to the crystallization of amorphous mullite in these coatings. To further verify that the coatings were crystallizing, the same mullite and composites samples were tested a second time; no discontinuous change in height at ~970°C was observed.

The measured values of the CTEs of each type of coating have been recorded in Table 3. The measured CTE for YSZ agrees with previously published values by Thurn et al.[25] However, data from Lee et al. gives a CTE of 5.4 x 10^{-6}/°C^{-1} for plasma sprayed mullite.[26] This discrepancy could be due to differences in the ratio of Al_2O_3 to SiO_2 in the mullites measured.[27] The measured CTE value for the YSZ/mullite composite was 6.4±0.5 x 10^{-6}/°C^{-1}. The calculated CTE value for the YSZ/mullite composite sample based on an upper bound rule of mixtures and the experimental values collected for pure mullite and YSZ coatings was 7.2 x 10^{-6}/°C^{-1}, which is close agreement with the experimental determined value.

(3) Compression Creep Behavior of Coatings

Overview: An overview of all creep tests conducted, the apparent steady-state strain rate, the total plastic strain that occurred during the creep test, and the number of replicates is given in Table 4. The apparent steady-state strain rates of each specimen were calculated from the slope of the linear portion of the creep data. All stand-alone coating specimens showed typical creep behavior with an initial elastic strain on loading followed by a transient, high-strain rate, region, and an apparent linear-steady state region. At the combined test temperature of ≥ 1100 °C and a

stress of ≥ 60 MPa, YSZ samples barreled during creep testing. YSZ samples tested at 1200°C and 80 MPa barreled then failed within the 5-hr test (see the top plot in Figure 5), exhibiting tertiary creep. Barreling in the YSZ specimens indicates a significant amount of friction between the load cell platens and the ends of the stand alone coating[28]. The effect of this friction on the present experimental data has not been determined. Barreling was not visually observed in composite or mullite specimens under the conditions investigated.

As shown in Figure 5, a comparison of the behavior of the coatings under 40, 60, and 80 MPa at 1200°C, increasing the applied stress on the coatings increased the total amount the specimens crept and the apparent steady-state creep rates in all coating types. For example, YSZ coatings tested at 1200°C exhibited a total creep strain of ~2.5%, ~4.0%, and ~6.3% (failed prior to 5 hrs) under stresses of 40, 60, and 80 MPa. From the results on YSZ, the threshold strain where barreling begins to occur is ~4%. Tests on mullite at 1200°C and compressive stresses of 40, 60, and 80 MPa conditions demonstrated a total strain of ~0.4%, ~0.6% and ~0.8 %, respectively. As is observed in Figure 5, the composite coating exhibited total creep deformation behavior that was more similar to mullite than YSZ. This was most evident in the composite coatings tested at 1200°C and 80 MPa where only ~2.3% deformation was observed during creep and no barreling was visually observed.

YSZ tested at 1200°C and stresses of 40, 60, and 80 MPa exhibited steady-state strain rates of ~7.2×10^{-7}, ~1.6×10^{-6}, and ~3.6×10^{-6} s^{-1}, respectively. Barreling would contribute to the latter two strain rates, resulting in higher rates than if only the YSZ was contributing to deformation. At the same test temperature, mullite samples demonstrated strain rates of ~7.0×10^{-8}, ~1.1×10^{-7}, and ~1.4×10^{-7} s^{-1} at applied stresses of 40, 60, and 80 MPa. These values were typically one order of magnitude less that those observed in the YSZ samples, and they showed

no evidence of barreling. Composite creep rates were generally closer to mullite creep rates than YSZ. For example, a composite specimen crept at 1200°C and 80 MPa displayed a creep rate of $6.7x10^{-7}$ s^{-1}.

Increasing test temperature resulted in a greater amount of creep and higher creep rates for all of the coating materials. YSZ coatings tested at 60 MPa at 1000°, 1100°, and 1200°C exhibited total deformations of ~ 0.33%, ~ 1.0%, and ~4.0 %, respectively. Mullite coatings tested under the same stress and temperatures exhibited total deformations of ~ 0.12%, ~ 0.24%, and ~0.58%, respectively. The creep strain observed in a composite sample at 1200°C and 60 MPa was ~1.6%, close to the value observed in mullite samples. Steady-state creep rates increased nearly two orders of magnitude from ~10^{-8} s^{-1} to ~10^{-6} s^{-1} from 1000° to 1200 °C in YSZ coatings tested at 60 MPa, but no more than one order of magnitude, from 10^{-8} s^{-1} to 10^{-7} s^{-1}, in mullite and composite coatings tested under the same conditions. It is important to realize that these results have not been normalized to account for differences in porosity between coating types. Thus, it does not appear that the greater porosity in the composite specimens was detrimental to its creep behavior when compared to the less porous YSZ specimens.

It is valuable to compare sintering rates of dense YSZ and mullite samples to the porous coatings investigated presently. Sudhir and Chokshi[29] investigated the compression creep characteristics of 8-mol% yttria-stabilized cubic zirconia. At 1400°C, the lowest temperature studied, and a compressive stress of 80 MPa, they observed a steady-state creep rate of 4 x 10^{-7} s^{-1}. As noted in Table 4, YSZ specimens tested at 1200°C and 80 MPa demonstrated a steady-state creep rate of 3.6 x 10^{-6} s^{-1}. While slight barreling of these samples may have artificially increased their strain rate, these coatings demonstrated comparable strain rates to dense YSZ but were tested at a 200°C lower temperature. In a study by Torrecillas et al.[30], dense mullite crept in

tension at 1200°C at 114 MPa demonstrated a steady-state creep rate of 5.3×10^{-9} s^{-1}. In the present study, mullite tested at 1200°C and 80 MPa displayed a steady-state creep rate in compression of 1.4×10^{-7} s^{-1}, substantially greater that of the dense mullite in tension. Thus, it is clear that the starting porosity, and presumably the reduction of this porosity during the test, is influencing the creep rates of the plasma-sprayed YSZ and mullite coatings. It is worth noting here that both studies referenced above were conducted on materials with approximately equiaxed grains. In the present study, the YSZ was composed of columnar grains and the mullite was likely composed of equiaxed grains as they nucleated and grew from the initially amorphous lamella during crystallization.

There has been some creep testing performed on mullite/zirconia composites, however, the test conditions and starting microstructures are vastly different than those evaluated in this study. For example, Descamps et al.[31] investigated the creep response of 70 vol.% mullite/30 vol.% zirconia composites in bending (tensile creep was reported) on samples prepared by reaction sintering of zircon and alumina using titania and magnesia additives. In these samples, the observed creep rates of 3×10^{-8} s^{-1} to 3×10^{-7} s^{-1} at 1200°C for an applied tensile stress of 80 MPa. These values were similar to those observed presently. In addition to the different stress state in the materials (i.e. tension creep in the cited study and compression creep presently), the microstructures of these materials were vastly different than those studied presently, with 1-5 μm diameter equiaxed zirconia grains in a mullite matrix observed.

In summary, all coatings demonstrated time-dependent creep behavior under the conditions tested, including an initial transient region followed by an apparent steady-state regime. Under the conditions tested only YSZ coatings failed when crept under a stress of 80 MPa at 1200°C. A 200°C increase in test temperature increased steady-state strain rates by

approximately two orders of magnitude, whereas an increase in applied stress of 40 MPa result in steady-state rates increasing by no more than one order of magnitude. The creep behavior of the composite specimens under any given combination of temperature and load stayed between that of the pure YSZ and pure mullite specimens.

Creep Activation Energies for the Coatings Investigated: The apparent steady-state strain rates of each specimen were used to determine the activation energies for creep for each coating type. As shown in Figure 6, activation energies were determined by measuring the slope of a line fit through data points on a plot of $\ln(\dot{\varepsilon})$ versus 1/T.

Two distinctive slopes (and therefore activation energies) were observed in the $\ln(\dot{\varepsilon})$ versus 1/T behavior of YSZ for each applied stress. For an applied stress of 80 MPa the activation energy was 410±40 kJ/mol between 1100^{o} and 1200^{o}C, and 164±40 kJ/mol between 1100^{o} and 1000^{o}C. As shown in Figure 6, similar behavior was observed for creep tests conducted at 40 and 60 MPa. There are two possible reasons for this behavior. As stated previously, barreling was observed at test temperatures ≥ 1100^{o}C and for stresses ≥ 60 MPa. As coatings barrel, significant bending stresses would increase the strain rate observed during individual tests. This would result in an apparent increase in activation energy and likely contribute to the activation energy differences observed presently, particularly in the 60 and 80 MPa data shown in Figure 6 for YSZ. However, no barreling was observed in the data collected at 40 MPa, yet the activation energy was not constant from 1000^{o} through 1200^{o}C. Erk et al.[32] have shown a transition in the mass transport phenomena in plasma-sprayed 7 wt.% YSZ coatings from surface diffusion dominant at 1000°C to volume diffusion dominant at temperatures of 1200°C and above. This may explain the observed change in the activation

energy.[32] At 1100°C, both volume and surface diffusion appear to be competing. Thus, the two activation energies observed in YSZ from 1000°-1100°C and from 1100°C -1200°C for a given stress level may be due to both barreling and a change in the transport mechanism.

The activation energies for mullite ranged from 122-156 kJ/mol between 1000°C and 1200°C, essentially independent of the applied stress. Within the error of the measurements, the same conclusion can be made regarding the activation energies of the YSZ/mullite composite samples. It should be noted that no change in the slope of the $\ln(\dot{\varepsilon})$ versus 1/T data was observed in the composite creep data, suggesting that the deformation mechanism(s) remained unchanged from 1000° through 1200°C and that the creep behavior of YSZ/mullite composites was dominated by the mullite phase.

Published creep studies on plasma-sprayed YSZ are limited [23,25,33,34,35]. Thurn et al.[25] measured an activation energy of 114 kJ/mol for air-plasma sprayed YSZ tested in compression using a set-up similar to that used in this study. The temperature range varied from 900° through 1100°C, and applied stresses ranged from 20-80 MPa. The reported activation energy by Thurn et al. is similar to that reported here, particularly for the data collected at 40 MPa. As is the present case, a portion of the creep strain was attributed to sintering of the coating. They also discuss that the load distribution in a plasma-sprayed coating is far from homogenous; rather, the combination of cracks and pores causes local stress concentrations that would result in localized strains.

No prior work citing creep studies of plasma-sprayed mullite were noted. Compression creep activation energies reported in the literature for mullite prepared using conventional powder processing techniques have typically been half those measured presently. A.R. de Arellan-Lopez et al.[36] measured an activation energy for compression loaded mullite of 385±20

kJ/mol between 1300°-1400°C and stresses of 7-15 MPa and noted that the activation energy is similar to that required for oxygen self-diffusion in mullite[37]. The samples in their study were 91% dense, but prior work on creep of ceramic materials indicated they did not significantly densify as a result of the applied stress[38]. However, in creep of plasma-sprayed YSZ, Thurn et al.[25] noted a 6% reduction in open porosity (from 22% to 16%) as a result of a compressive creep strain of 1%. In the samples tested presently, the porosity of plasma-sprayed mullite was ~21%, and it is thought that densification during the creep test may explain differences in the activation energy.

Stress relaxation experiments on plasma-sprayed YSZ cylinders[12] have revealed deformation mechanisms that are likely similar to those experienced during creep. YSZ has been shown to relax uniaxial compressive stresses in two stages. In the first stage of relaxation, stress is relieved by the initiation and growth of cracks parallel to the applied load, the sliding of lamellae and their compaction, and the healing of cracks perpendicular to the applied load. It is worth noting that most of the relaxation in stage I comes from altering the microstructural features intrinsic to the plasma-sprayed coating. In the second stage relaxation is slower, and research indicates that relaxation is due the inherent properties of the ceramic through grain boundary sliding and diffusion with contributions from densification are likely[12,13]. It has been suggested that the deformation mechanisms of the second stage of relaxation are the same as those during steady-state creep.

In the present study, the continuous mullite phase clearly dominates the steady state-creep rate in the composite samples. As the materials response in the steady-state creep regime is dominated by the intrinsic properties of the ceramic material as opposed to the distinct microstructural features of the plasma-sprayed coating, it appears that the improved creep

resistance of the mullite/YSZ composite is due to the inherent creep resistance of the mullite phase.

IV. Summary

The thermal expansion and creep behavior of stand-alone coatings of 7 wt.% Y_2O_3-ZrO_2, mullite, and a 45:55 volume ratio composite of YSZ:mullite were characterized. Cylindrical coatings were subject to uniaxial compression creep tests under stresses ranging from 40-80 MPa for 5 hours at temperatures between 1000° and 1200°C. Overall, the YSZ/mullite composite showed improved creep resistance over YSZ-only coatings and should be investigated further for its possible use in thermal barrier coating systems. However, the addition of mullite to YSZ in the composite specimens reduced the CTE of YSZ, which could be detrimental to the lifetime of the composite as a TBC.

References

[1] D. R. Clarke and C. G. Levi, "Materials Design for the Next Generation Thermal Barrier Coatings," *Annu. Rev. Mater. Res.*, **33** 383-417 (2003).

[2] P. Ramaswamy, S. Seetheramu, K. B. R. Varma, N. Raman and K. J. Rao, "Thermomechanical Fatigue Characterization of ZrO_2 and Mullite Thermal Barrier Coatings on Diesel Engine Components: Effect of Coatings on Engine Performance." Proc. Instn. Mech. Engrs. Part C, *J. Mech Sci.*, **214** [5] 729-42 (2000).

[3] R. A. Miller, S. R. Levine and P. E. Hodge, "Thermal Barrier Coatings for Superalloys." *Proc. 4th Int. Symp. On Superalloys, Seven Springs,* PA, September 21-25, 1980, American Society for Metals, Metals Park, OH, 1980, pp. 473-480.

[4] W. Beele, G. Marijnissen, and A. Van Lieshout, "The Evolution of Thermal Barrier Coatings—Status and Upcoming Solutions for Today's Key Issues," *Surf. Coat. Tech.*, **120** 61-7 (1999).

[5] R.A. Miller, "Current Status of Thermal Barrier Coatings—An Overview," *Surf. Coat. Tech.*, **30** 1-11 (1987).

[6] R. McPherson, "A Review of Microstructure and Properties of Plasma Sprayed Ceramic Coatings," *Surf. Coat. Tech*., **39/40** 173-181 (1989).

[7] R. McPherson, "The Relationship Between Mechanism of Formation, Microstructure and Properties of Plasma-Sprayed Coatings," *Thin Solid Films*, **83** 297-310 (1981).

[8] R.A. Miller and C.E. Lowell, "Failure Mechanisms of Thermal Barrier Coatings Exposed to Elevated Temperatures," *Thin Solid Films*, **95** 265-273 (1982).

[9] R.A. Miller, "Thermal Barrier Coatings for Aircraft Engines—History and Direction," *J. Therm. Spray Tech.*, **6** [1] 35-42 (1997).

[10] J. Ilavsky, J. K. Stalick, "Phase Composition and Its Changes During Annealing of Plasma-Sprayed YSZ," Surf. Coat. Tech., **127** 120-129 (2000).

[11] K. Kokini, A. Banerjee, and T. A. Taylor, "Thermal Fracture of Interfaces in Pre-Cracked Thermal Barrier Coatings," *Mat. Sci. Engr. A,* **A323** 70-82 (2002).

[12] G. R. Dickinson, C. A. Petorak, K. Bowman and R.W. Trice, "Stress Relaxation of Compression Loaded Plasma-Sprayed 7 Wt% Y_2O_3-ZrO_2 Stand-Alone Coatings," *J. Am. Ceram. Soc.*, **88** [8] 2202-8 (2005).

[13] Petorak, C. A. "High Temperature Mechanical Behavior of Plasma-Sprayed 7wt,% Yttria-Stabilized Zirconia Stand-Alone Coatings" Thesis. Purdue University. June 2005.

[14] E. F. Rejda, D. F. Socie and T. Itoh, "Deformation Behavior of Plasma-Sprayed Thick Thermal Barrier Coatings," *Surf. Coat. Tech.*, **113** 218-226 (1999).

[15] K. Kokini, Y. R. Takeuchi and B. D. Choules, "Surface Thermal Cracking of Thermal Barrier Coatings Owing to Stress Relaxation: Zirconia vs Mullite," *Surf. Coat. Tech.*, **82** 77-82 (1996).

[16] B. D. Choules, K. Kokini and T. A. Taylor, "Thermal Fracture of Ceramic Thermal Barrier Coatings Under Heat Flux With Time-Dependent Behavior. Part 1. Experimental Results," *Mat. Sci. Engr.*, **A299** 296-304 (2001).

[17] W. D. Kingery, H. K. Bowen and D. R. Uhlmann, *Introduction to Ceramics*, 2nd ed.; pp. 240, 595, 304 and 642. Wiley, New York, 1976.

[18] P.A. Lessing, R.S. Gordon, and K.S. Mazdiyasni, "Creep of Polycrystalline Mullite," J. Am. Ceram. Soc., **58** [3-4] 149 (1975).

[19] P.C. Dokko, J.A. Pask, and K.S. Mazdiyasni, "High-Temperature Mechanical Properties of Mullite Under Compression," J. Am. Ceram. Soc., **60** [3-4] 150-155 (1977).

[20] C. K. Yoon and I. W. Chen, "Superplastic Flow of Two-Phase Ceramics Containing Rigid Inclusions—Zirconia/ Mullite Composites," *J. Am. Ceram. Soc.*, **73** [6] 1555-1565 (1990).

[21] W. E. Lee and W. M. Rainforth, *Ceramic Microstructures: Property Control by Processing*; p. 310. Chapman and Hall, New York, 1994.

[22] J.B. Wachtman, *Mechanical Properties of Ceramics*; p. 392. Wiley, New York, 1996.

[23] H. Echsler, D. Renusch, and M. Schutze, "Mechanical Behavior of As Sprayed and Sintered Air Plasma Sprayed Partially Stabilized Zirconia," Mat. Sci. Tech., **20** 869-876 (2004).

[24] K. Bowman, "Mechanical Behavior of Materials," John Wiley and Sons, Inc. (2004).

[25] G. Thurn, G. A. Schneider and F. Aldinger, "High-Temperature Deformation of Plasma-Sprayed ZrO_2 Thermal Barrier Coatings," *Mat. Sci. Engr. **A*** **233** 176-182 (1997).

[26] K. N. Lee, R.A. Miller and N.S. Jacobson, "New Generation of Plasma-Sprayed Mullite Coatings on Silicon Carbide," *J. Am. Ceram. Soc.* **78** [3] 705-710 (1995).

[27] H. Schneider, K. Okada and J. A. Pask, *Mullite and Mullite Ceramics*, pp. 224-225. John Wiley & Sons, New York, 1994.

[28] K.D. Debschutz, B. Caspers, G.A. Schneider, and G. Petzow, "Critical Evaluation of the Compression Test," J. Am. Ceram. Soc., **76** [10] 2468-74 (1993).

[29] B. Sudhir and A. Chokshi, "Compression Creep Characteristics of 8-mol%-Yttria-Stabilized Cubic-Zirconia," J. Am. Ceram. Soc., **84** [11] 2625-32 (2001).

[30] R. Torrecillas, G. Fantozzi, S. de Aza and J. S. Moya, "Thermomechanical Behavior of Mullite," *Acta Mater.* **45** [3] 897-906 (1997).

[31] P. Descamps, S. Sakaguchi, M. Poorteman, and F. Cambier, "High-Temperature Characterization of Reaction Sintered Mullite-Zirconia Composites," J. Am. Ceram. Soc., **74** [10] 2476-81 (1991).

[32] K. A. Erk, C. Deschaseaux and R. W. Trice, "Grain Boundary Grooving of Plasma-Sprayed Yttria-Stabilized Zirconia Thermal Barrier Coatings," *J. Am. Ceram. Soc.*, IN PRESS.

[33] M. Ahrens, S. Lampenscherf, R. Vassen, and D. Stover, "Sintering and Creep Responses in Plasma-Sprayed Thermal Barrier Coatings," J. Therm. Spray Techn., **13** [3] 2004.

[34] D. Zhu, and R. Miller, "Sintering and Creep Behavior of Plasma-Sprayed Zirconia- and Hafnia-Based Thermal Barrier Coatings," Surf. Coat. Techn., **108-109** 114-20 (1998).

[35] D. Zhu and R. Miller, "Determination of Creep Behavior of Thermal Barrier Coatings Under Laser Imposed Temperature and Stress Gradients," NASA Technical Memorandum 113169, Lewis Research Center, Nov. 1997.

[36] A.R. de Arellano-Lopez, J.J. Melendez-Martinez, T.A. Cruse, R.E. Koritala, J.L. Routbort, and K.C. Goretta, "Compressive Creep of Mullite Containing Y_2O_3," Acta Materialia 50 4325-4338 (2002).

[37] Y. Ikuma, E. Shimada, S. Sakano, M. Oishi, M. Yokoyama, Z. Nakagawa, "Oxygen Self-Diffusion in Cylindrical Single-Crystal Mullite" J. Electrochem Soc., **146** [12] 4672-4675 (1999).

[38] J.M. Calderon-Moreno, R. Torrecillas, "High Temperature Creep of Polycrystalline Mullite", Key Eng. Mater **132-136** 587-90 (1997).

Table 1: Comparison of Thermal Behavior of Dense YSZ and Mullite.[17]

Material	CTE ($*10^{-6}$/K)	Melting Temp. (ºC)	k_{th} at 1000 ºC (W/m/K)
YSZ	10.0	~2700	2.3
Mullite	5.3	1828	3.7

Table 2: Average Densities and Thicknesses of As-Sprayed Coatings.

Material	Bulk Density (g/cm^3)	Theoretical Density (g/cm^3)	Total Porosity (%)	Thickness (μm)
YSZ	5.2±0.2	6.08	14.5±3.0	650
Composite	3.6±0.1	4.51*	19.8±2.0	670
Mullite	2.5±0.1	3.18	21.4±3.0	630

*calculated using rule of mixtures based on 54 vol. % mullite/45 vol.% YSZ

Table 3: Measured Coefficients of Thermal Expansion for YSZ, Composite, and Mullite Specimens.

Material	Average CTE (1/ºC)$*10^{-6}$
YSZ	11.0 ± 0.6
Composite	6.4 ± 0.5
Mullite	4.0 ± 0.2

Table 4: Overview of All Creep Tests on YSZ, Composite, and Mullite Samples.

Specimen	Stress, MPa	Temp., ^{o}C	Compressive Strain Rate, s^{-1}	Total Compressive Creep Strain, %	Replicates
YSZ	40	1000	$5.9\times10^{-8}\pm1.6\times10^{-8}$	0.34±0.09	4
YSZ	40	1050	7.5×10^{-8}	0.39	1
YSZ	40	1100	1.6×10^{-7}	0.80	1
YSZ	40	1150	3.3×10^{-7}	1.36	1
YSZ	40	1200	$7.2\times10^{-7}\pm3.0\times10^{-8}$	2.46±0.10	3
YSZ	60	1000	$6.2\times10^{-8}\pm5.5\times10^{-9}$	0.33±0.01	2
YSZ	60	1050	1.1×10^{-7}	0.57	1
YSZ	60	1100	2.1×10^{-7}	0.98	1
YSZ	60	1150	5.5×10^{-7}	1.98	1
YSZ	60	1200	$1.6\times10^{-6}\pm4.4\times10^{-7}$	4.00	2
YSZ	80	1000	$1.0\times10^{-7}\pm5.0\times10^{-9}$	0.58±0.00	2
YSZ	80	1050	1.4×10^{-7}	0.70	1
YSZ	80	1100	3.3×10^{-7}	1.50	1
YSZ	80	1150	8.2×10^{-7}	2.74	1
YSZ	80	1200	$3.6\times10^{-6}\pm3.5\times10^{-7}$	6.25±0.08[a]	2
Composite	40	1000	$3.0\times10^{-8}\pm9.2\times10^{-9}$	0.21±0.05	7
Composite	40	1100	1.0×10^{-7}	0.60	1
Composite	40	1200	$2.5\times10^{-7}\pm2.7\times10^{-8}$	1.27±0.13	3
Composite	60	1000	$4.9\times10^{-8}\pm1.2\times10^{-8}$	0.28±0.06	2
Composite	60	1100	1.4×10^{-7}	0.75	1
Composite	60	1200	3.7×10^{-7}	1.61	1
Composite	80	1000	$5.5\times10^{-8}\pm1.7\times10^{-8}$	0.33±0.13	3
Composite	80	1100	$2.0\times10^{-7}\pm4.5\times10^{-8}$	1.02±0.23	3
Composite	80	1200	6.7×10^{-7}	2.33	1
Mullite	40	1000	$1.5\times10^{-8}\pm2.5\times10^{-9}$	0.10±0.03	3
Mullite	40	1100	4.0×10^{-8}	0.24	1
Mullite	40	1200	$7.0\times10^{-8}\pm3.0\times10^{-9}$	0.41±0.02	3
Mullite	60	1000	1.5×10^{-8}	0.12	1
Mullite	60	1100	4.6×10^{-8}	0.24	1
Mullite	60	1200	$1.1\times10^{-7}\pm1.4\times10^{-8}$	0.58±0.08	2
Mullite	80	1000	2.3×10^{-8}	0.11	1
Mullite	80	1100	6.2×10^{-8}	0.33	1
Mullite	80	1200	1.4×10^{-7}	0.76	1

Figure Captions

Figure 1: Back-scatter SEM micrograph of an as-sprayed composite coating taken at random location in the composite coating showing a 45:55 volume ratio of YSZ (white) to mullite (grey).

Figure 2: SEM micrographs of fracture surfaces of (a) YSZ, (b) YSZ/mullite composite, and (c) mullite as-sprayed coatings. The YSZ phase appears as lamella structures, with columnar grains apparent. The mullite phase appears glassy. Porosity is apparent in both phases.

Figure 3: XRD analysis of as-sprayed (top) and heat treated mullite specimens (50-hr at 1400°C) (bottom) showing the glassy nature of mullite in the as-sprayed condition and subsequent crystallization during heat treatment.

Figure 4: Linear change versus temperature for YSZ, mullite, and composite specimens. The YSZ shows linear behavior over the entire temperature range, while mullite and composite specimens only showed linear behavior over a limited range of temperatures. A drastic increase in shrinkage of the coatings containing mullite occurs at 970 ºC associated with the crystallization of mullite.

Figure 5: Representative comparison of the creep behavior of YSZ, mullite, and composite coatings at 1200 °C under 40, 60 and 80 MPa. The behavior of the composite was consistently in between that of the mullite and YSZ coatings. YSZ coatings failed under 80 MPa and barreled under 60 MPa loads at this temperature. Note that the elastic response for each sample was subtracted from this data.

Figure 6: Plot of natural log of steady-state strain rate versus one over absolute temperature of YSZ, mullite and the YSZ/mullite composite coatings tested under constant load.

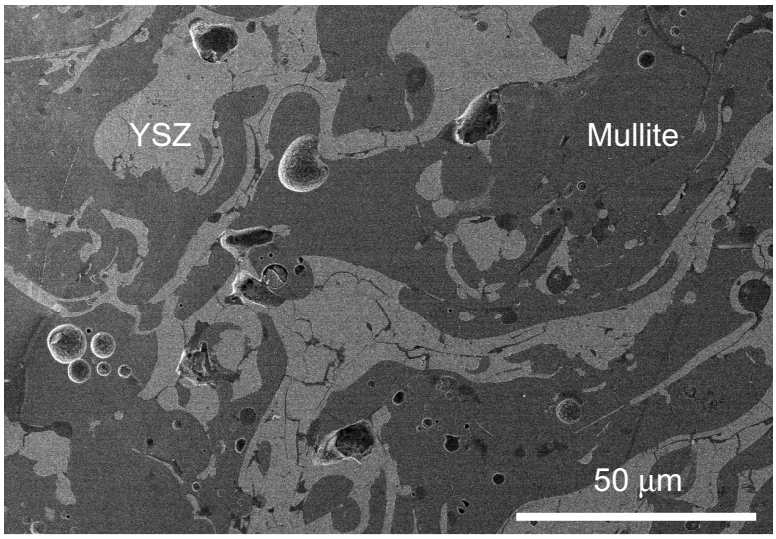

Figure 1

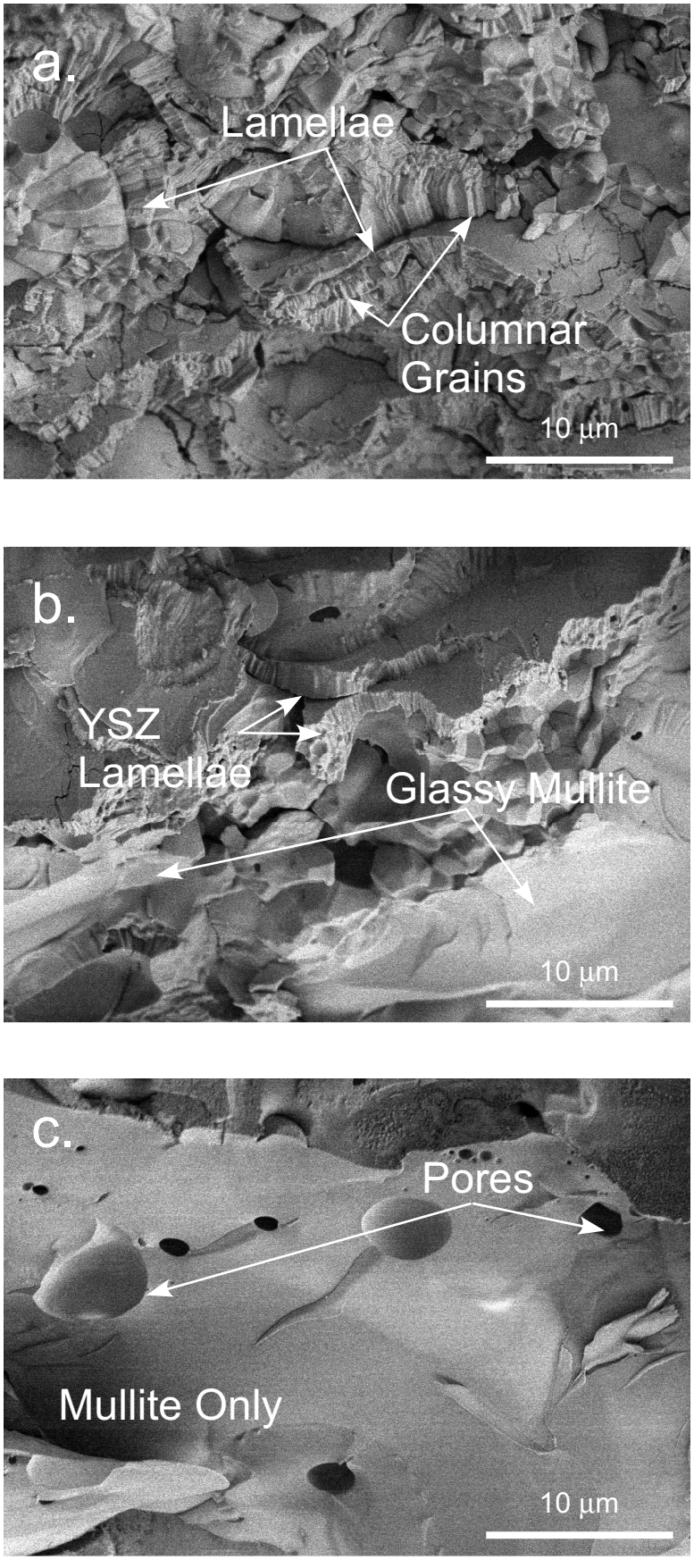
a.
Lamellae
Columnar
Grains
10 µm
b.
YSZ
Lamellae
Glassy Mullite
10 µm
c.
Pores
Mullite Only
10 µm

Figure 2

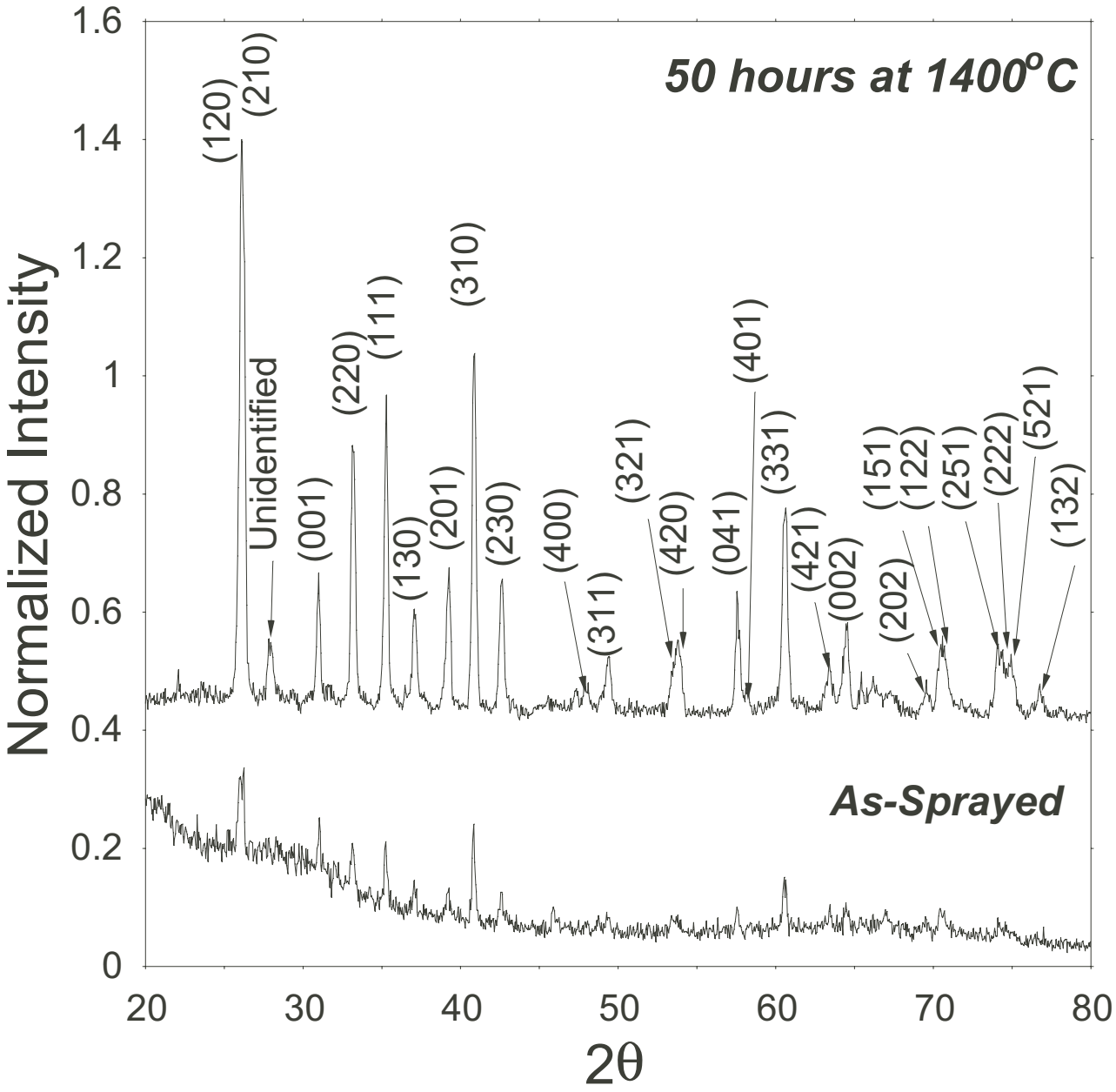
50 hours at 1400°C
As-Sprayed
Normalized Intensity
2θ
(120)
(210)
Unidentified
(001)
(220)
(111)
(130)
(201)
(310)
(230)
(400)
(311)
(321)
(420)
(041)
(401)
(331)
(421)
(002)
(202)
(151)
(122)
(251)
(222)
(521)
(132)

Figure 3

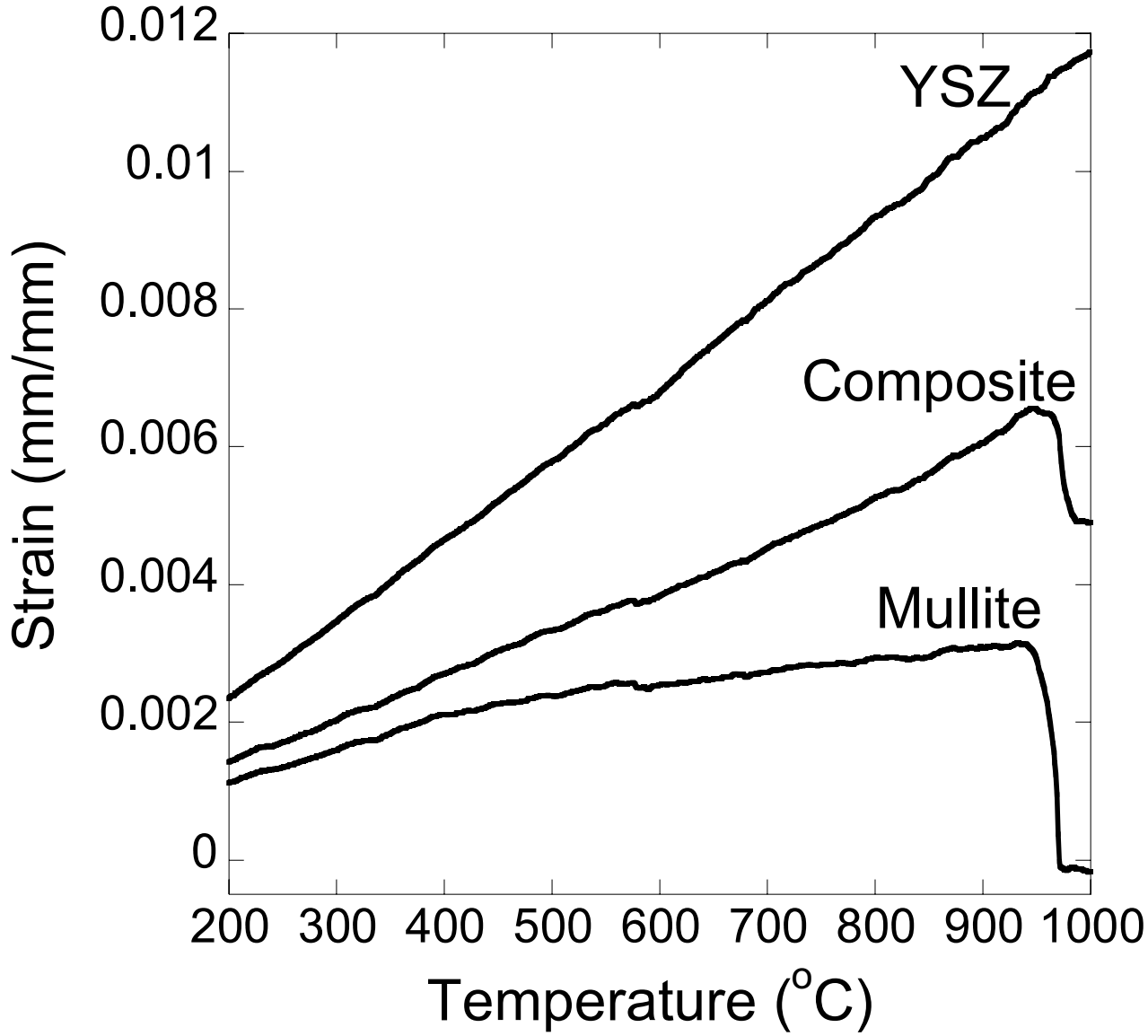
0.012
0.01
0.008
0.006
0.004
0.002
0
Strain (mm/mm)
YSZ
Composite
Mullite
200 300 400 500 600 700 800 900 1000
Temperature (°C)

Figure 4

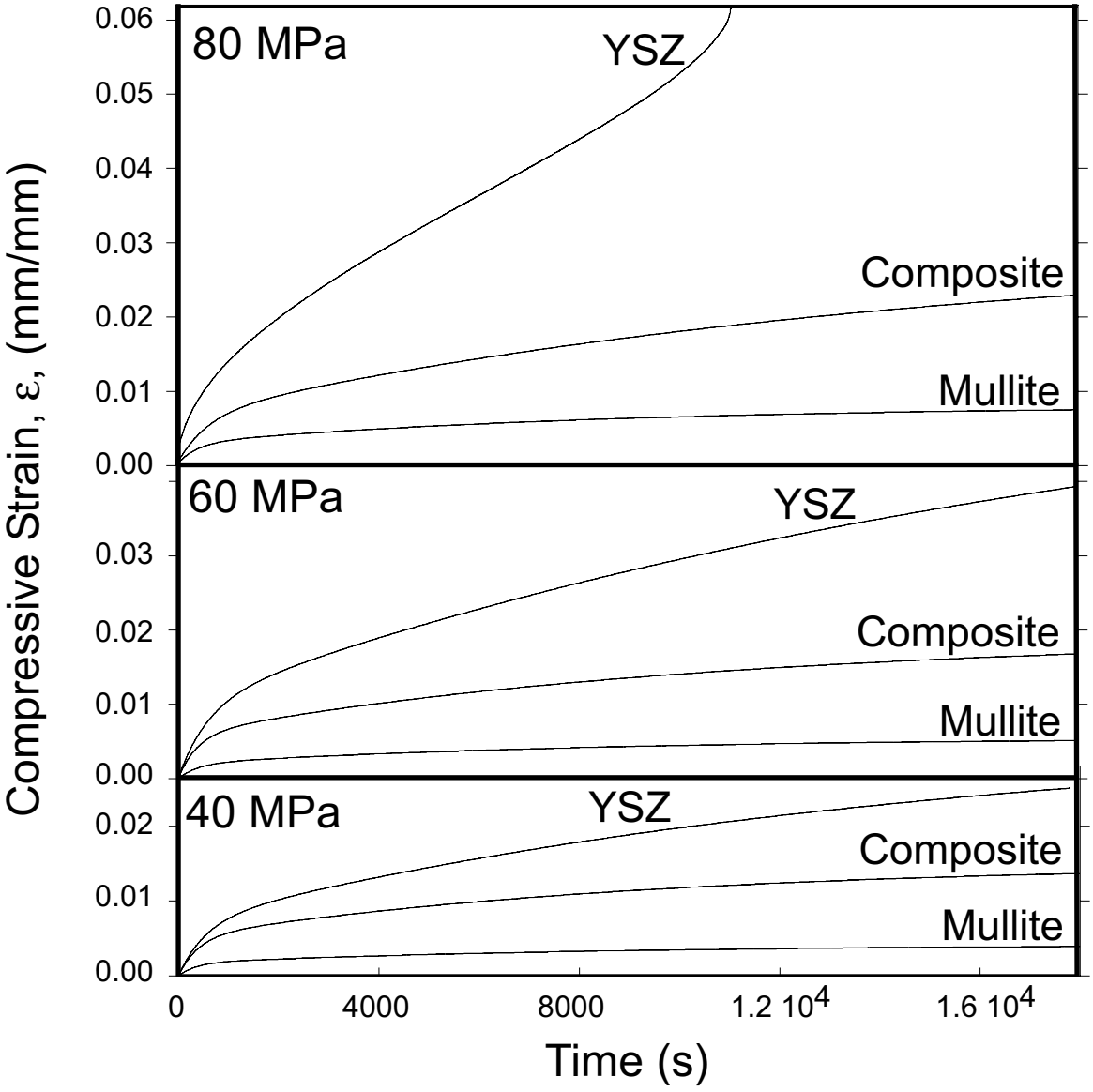
80 MPa
YSZ
Composite
Mullite
60 MPa
YSZ
Composite
Mullite
40 MPa
YSZ
Composite
Mullite
Compressive Strain, ε, (mm/mm)
0.06
0.05
0.04
0.03
0.02
0.01
0.00
0.03
0.02
0.01
0.00
0.02
0.01
0.00
0
4000
8000
1.2 10^4
1.6 10^4
Time (s)

Figure 5

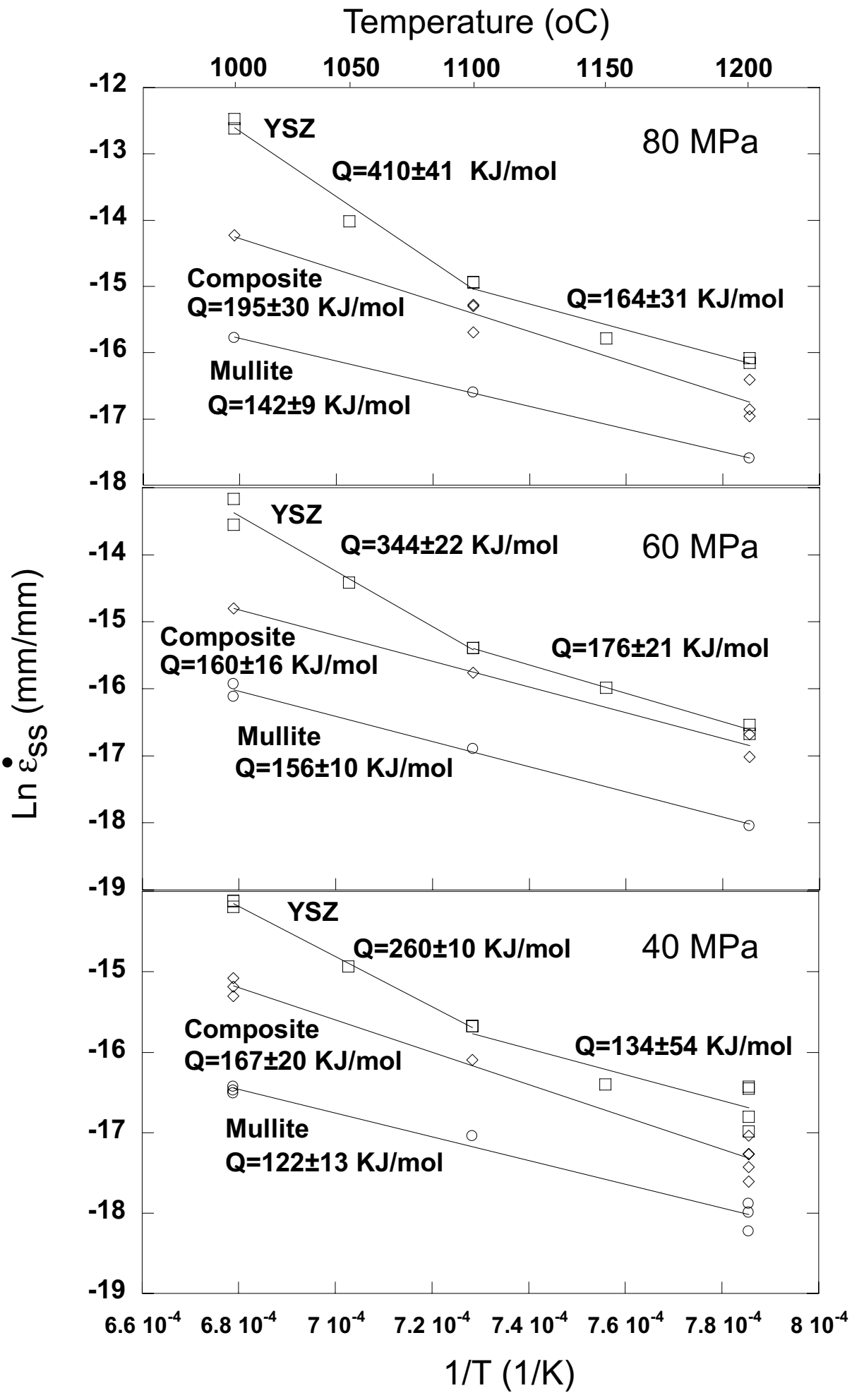
Temperature (oC)
1000
1050
1100
1150
1200
-12
-13
-14
-15
-16
-17
-18
-19
YSZ
80 MPa
Q=410±41 KJ/mol
Composite
Q=195±30 KJ/mol
Q=164±31 KJ/mol
Mullite
Q=142±9 KJ/mol
YSZ
60 MPa
Q=344±22 KJ/mol
Composite
Q=160±16 KJ/mol
Q=176±21 KJ/mol
Mullite
Q=156±10 KJ/mol
YSZ
40 MPa
Q=260±10 KJ/mol
Composite
Q=167±20 KJ/mol
Q=134±54 KJ/mol
Mullite
Q=122±13 KJ/mol
Ln ε̇ss (mm/mm)
6.6 10-4
6.8 10-4
7 10-4
7.2 10-4
7.4 10-4
7.6 10-4
7.8 10-4
8 10-4
1/T (1/K)

Figure 6